Current-driven hysteresis effects in manganite spintronics devices

I. Pallecchi*
CNR-INFM LAMIA, Corso Perrone 24, 16152 Genova, Italy

L. Pellegrino
Dipartimento di Fisica, Università di Genova, Via Dodecaneso 33, 16146 Genova, Italy and CNR-INFM LAMIA, Corso Perrone 24, 16152 Genova, Italy

A. Caviglia
Dipartimento di Fisica, Università di Genova, Via Dodecaneso 33, 16146 Genova, Italy

E. Bellingeri
CNR-INFM LAMIA, Corso Perrone 24, 16152 Genova, Italy

G. Canu
Dipartimento di Fisica, Università di Genova, Via Dodecaneso 33, 16146 Genova, Italy

G. C. Gazzadi
CNR-INFM-National Research Center on nanoStructures and bioSystems at Surfaces-S3, Via G. Campi 213/A-41100 Modena, Italy

A. S. Siri and D. Marré
CNR-INFM LAMIA and Università di Genova, Corso Perrone 24, 16152 Genova, Italy
(Received 11 April 2006; revised manuscript received 6 June 2006; published 26 July 2006)

By carrying out differential resistance measurements in oxygen deficient $La_{0.67}Ba_{0.33}MnO_{3-\delta}$ thin films at different magnetic fields, in submicrometric constricted regions patterned by focused ion beam, we find evidence of hysteretic resistance behavior as a function of both the external magnetic field and dc bias current. The resistance curves exhibit a marked asymmetry with respect to the polarity of the current. We suggest that the spin-polarized injected current exerts a torque on magnetic domains, whose rotation accounts for the hysteretic resistance changes. The memory effect of such constrictions is potentially interesting both for studying micromagnetic effects and in view of spintronics devices applications.

DOI: 10.1103/PhysRevB.74.014434 PACS number(s): 75.47.Lx, 85.75.Dd, 72.25.Mk

I. INTRODUCTION

Manganite perovskites are unique systems due to their highly spin-polarized current,[1] their colossal magnetoresistance, and their Curie temperature above room temperature, which makes them appealing candidates for fundamental studies as well as for spintronics applications. Furthermore, their perovskite crystal structure common to other functional oxides, such as high-T_c superconducting cuprates and ferroelectric titanates, allows the growth of epitaxial heterostructures and the realization of novel devices.

Magnetic hysteresis in manganite thin films has been exploited to realize spin valves in stacked layers geometry.[1–7] Among spintronics prototype devices, planar constrictions have been investigated both for their enhanced magnetoresistance,[8,9] their effectiveness in pinning magnetic domain walls,[10,8] as well as for planar spin valve effect.[11–13] Geometrically constrained magnetic walls can be used as tunneling barriers, whose conductance and magnetoconductance can be well controlled by the geometrical parameters of the system. In addition, narrow channels offer the possibility of studying mesoscopic magnetic systems where a small number of magnetic domain is present. In these conditions, the effects of the external magnetic field and injected nonpolarized or spin-polarized current on the domains configuration can be inspected more easily.[11]

As a consequence of the strong interplay between magnetic, transport, and lattice degrees of freedom, manifold effects related to electric current and electric field have been observed in manganites: electric-field-induced lattice distortions causing resistance modulation,[14] spin polarized carriers injection,[15] current induced electrostrictive irreversible effects,[16] tuning of the metal-insulator transition by field effect[17] and by ferroelectric field effect.[18]

A class of experiments has reported on resistive switching induced by voltage pulses in systems containing strongly correlated perovskite oxides and, in particular, narrow bandwidth semiconducting manganites;[19] these nonvolatile reversible resistive states are thought not to be related to the intrinsic behavior of bulk manganites, but rather to be characteristic of metal-oxide interfacial layers, as they have been observed in two-leads measurements, but not in four-leads measurements. They have been attributed to pulse driven changes in traps density.[19] However, nucleation of ferromagnetic metallic clusters triggered by the electric field has also been proposed as an explanation.[20] Electroresistive hysteretic effects in two-leads measurements have been recently studied in Schottky barriers at metal-manganite interfaces.[21]

Even more interesting is the study of intrinsic mechanisms. Hysteretic jumps in current-voltage characteristics occurring above a certain threshold current or voltage in manganite samples have been reported by several authors[22–30] and proposed for applications as memory devices. A collapse of the charge-ordered phase due to electrical current and formation of ferromagnetic conducting paths has been proposed as an explanation;[24,25,30] also the possibility of modifying the spatial orientation of anisotropic shaped *d* orbitals by an electric field has been evidenced.[31,25] Similar phenomenology has been found also in non-charge-ordered manganites; in this case, the role of the electric field in altering the spatial distribution of charge in MnO_6 octahedra, thus favoring the double-exchange transfer of charge carriers and enhancing conductivity, has been invoked.[27] Other authors claim that Joule heating associated with current flow through localized pathways of ferromagnetic clusters in phase-separated manganites could account for hysteretic resistivity jumps,[29] but bistable resistance states caused by Joule self-heating have been also observed in non-phase-separated manganites.[32] In all these experiments, the effect of the magnetic field has been very different: it was observed either to decrease the threshold current-voltage,[24] or increase it,[23] or have almost no effect[27] or else increase the hysteresis of the current-voltage characteristics.[28] Yuzhelevski *et al.*[22] examined the behavior of metastable resistivity states in low doped manganites and tentatively concluded that they could be related to switching of magnetic moments between parallel and antiparallel orientations induced by the spin-polarized current. In this scenario, the smallness of the observed threshold current as compared to cobalt-based spin-transfer systems has been ascribed to the low magnetic anisotropy constant as well as to the percolative nature of the current path. Also, Sun[23] has explicitly invoked the transfer of spin momentum to account for steps in asymmetric and hysteretic *I-V* characteristics in manganite junctions. Finally, the current dependence of the measured resistance of manganite epitaxial films has been explained in terms of Joule heating, but also a spin-transfer mechanism has been considered by Gao *et al.*[33]

Experimental evidences of spin torque have been widely studied in cobalt-based trilayers[34,35] and pillars[36] and theoretical approaches to this mechanism have been developed in Refs. 37 and 38.

Magnetization switching in spintronic devices is typically driven by a suitable external magnetic field. On the other hand, it has been predicted that, while an electric current exerts a force on domain walls via exchange coupling,[39] a spin-polarized current exerts a torque on the wall magnetization.[40] In other words, a spin-polarized current exerts a torque on the local magnetic domain, due to local exchange interactions between conduction electrons and magnetic moments. By applying angular momentum conservation during scattering of spin-polarized electrons from magnetic interfaces, the expression for the torque associated with vectorial spin transfer is obtained.[41] It follows that an applied current can be used to flip adjacent magnetic domains of different orientation. In this mechanism there is an asymmetry in terms of direction of bias current: two adjacent magnetic domains can be aligned antiparallel by currents flowing in one direction and parallel by currents flowing in the opposite direction. An intuitive explanation for the torque direction is the following. If spin-polarized electrons are emitted from a ferromagnetic electrode having fixed magnetization direction, that is a larger coercive field, into an adjacent ferromagnetic electrode having a smaller coercive field, the latter experiences a torque toward the direction of the emitting electrode. The opposite situation occurs if the emitting electrode has the smaller coercive field: the emitting electrode is depleted of electrons polarized along the magnetization direction of the collecting electrode, which have the largest transmission probability with respect to otherwise polarized electrons; this is equivalent to a torque that rotates the average magnetization direction of the emitting electrode away from the direction of the collecting electrode magnetization. Thereby, for a given direction of the current flow, the parallel or antiparalled configuration is stabilized depending on whether the emitting electrode has a larger or smaller coercive field than the collecting electrode, respectively.

In a previous paper, we have shown the possibility of fabricating planar spin valves in manganite epitaxial films, whose hysteretic resistance associated with domain orientation is controlled by the external magnetic field.[11] The magnetization reversal, resulting from the competition between the Zeeman energy trying to expand the size of the reversed domain and the domain wall energy trying to reduce the length of the domain wall, was monitored in resistance versus magnetic field measurement, by sweeping the external field parallel to the film surface. In the present paper we demonstrate that planar spin devices fabricated by focused ion beam (FIB) in low doped manganites exhibit hysteretic resistance, which is controlled by an injected spin-polarized current. In this case, rotation of the local magnetization is monitored by sweeping the applied dc spin-polarized current.

II. EXPERIMENTAL

$La_{0.67}Ba_{0.33}MnO_{3-\delta}$ thin films are deposited by pulsed laser ablation on $SrTiO_3$ substrates in low oxygen pressure at 800 °C. The structural and electrical properties of the films are checked by x-ray diffraction and resistance versus temperature curves, measured by a standard four-probe technique. The films turn out to be metallic below a transition temperature which varies in the range 150–250 K, depending on the oxygen content of the film. A low-temperature upturn in the less oxygenated samples occurs. Mesas with pads for bonded electrical contacts are patterned by optical lithography and wet etching in HCl. Submicrometric constrictions of 0.1–1 μm width are patterned by FIB. This technique enables direct, maskless fabrication of submicron and nanometer sized structures by sputtering removal of the top layer with a high resolution (<10 nm) ion beam, similarly to the procedure described in Ref. 12. A dual beam system (FEI DB235M), combining a Ga^+ FIB and a scanning electron microscope (SEM) is employed, allowing *in situ* inspection of the fabricated constrictions. A SEM image of one of such constrictions is shown in the inset of Fig. 1.

Four-probe current-voltage characteristics at different magnetic fields parallel to the film plane are measured both in dc and ac regimes. In the latter case a lock-in amplifier is used with a dc bias current superimposed to an ac oscillatory current of low frequency (23 Hz is chosen).

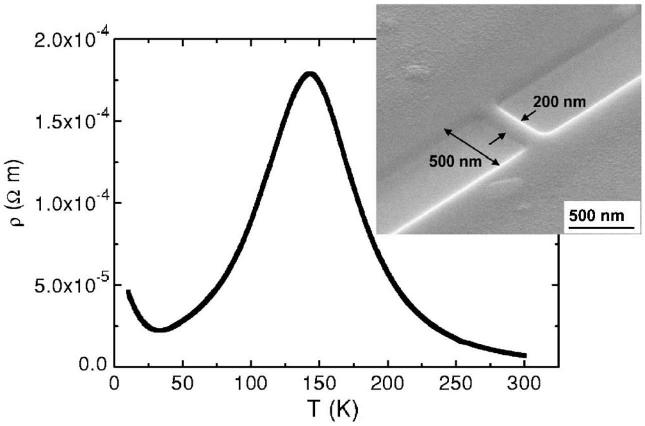

FIG. 1. Resistivity vs temperature measurement of one of the constrictions whose ac resistance measurements are presented in the paper. Inset: SEM image of a 200 nm wide constriction, patterned by FIB.

III. RESULTS AND DISCUSSION

In Fig. 1, the resistivity versus temperature curve of a constriction in an 80-nm-thick oxygen deficient film is shown, with a metal-insulator transition temperature of about 140 K and an upturn below 30 K. Below the transition temperature, transport occurs across a percolation path of ferromagnetic clusters. The low-temperature reentrant insulating state is commonly observed in low doped manganites and is usually associated with tunneling across intrinsic weak links or depletion layers in the vicinity of grain boundaries.[42,22] We note that the resistivity curve of the constriction is almost identical to that of unconstricted areas apart from a scale factor corresponding to the cross section. This demonstrates the microscopic homogeneity of the sample as well as the fact that optical lithography, wet etching, and FIB patterning do not deteriorate the sample quality.

In Fig. 2(a), curves of the voltage-current derivative dV/dI as a function of the superimposed dc bias current measured on a typical constriction at different magnetic fields and at 10 K are shown. At low dc current bias, the dV/dI curves tend to diverge. This effect is also observed as a small discontinuity in the dc I-V characteristics close to zero bias current (see Fig. 6 and the discussion later on). Low bias discontinuities have been observed in low doped manganites by other authors.[28,29,21] Such sharp steps are independent of the magnetic field and are probably related to Schottky barriers at the electrical contacts between the aluminum wires and the manganite film, which are not perfectly identical to one another. Indeed, the formation of a Schottky barrier is expected between a metal with low work function and a hole doped material, and its width and height are determined by the local hole concentration. However, we think that this effect is not related to the physics of the hysteretic resistivity jumps studied hereafter (the zero bias anomaly is seen also in samples where no hysteretic jumps are observed) and we will not discuss it further in the remainder of this paper. At low temperature, the ac resistance measurements of the constrictions present irregular but reproducible features for one sign of the dc bias current. For example, in the curves

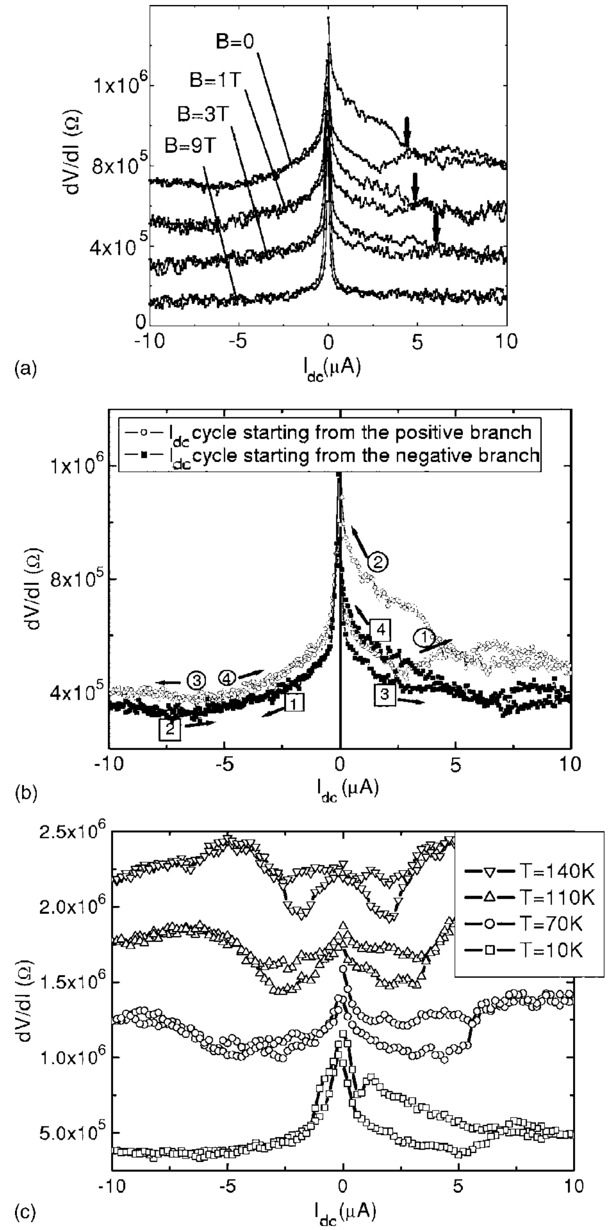

FIG. 2. (a) Differential resistance dV/dI characteristics as a function of the superimposed dc bias current (which is cycled from zero, to its maximum positive value, then to its maximum negative value, then again to zero) measured at different magnetic fields and at temperature 10 K in a typical constriction. The black arrows roughly indicate the threshold current for the onset of hysteretic features. The curves are shifted by a constant offset for clarity. (b) Differential resistance dV/dI characteristics as a function of the superimposed dc bias current measured in the same constriction in zero magnetic field at 10 K, by sweeping either the positive current branch first (open circles) or the negative current branch first (filled squares); the numbers in the circles/squares from 1 to 4 and the black arrows indicate the temporal succession of the branches and the direction of the current sweep for each branch. (c) Differential resistance dV/dI characteristics as a function of the superimposed dc bias current measured in the same constriction in zero magnetic field at different temperatures; the black arrows roughly indicate the threshold current for the onset of hysteretic features. The curves are shifted by a constant offset for clarity.

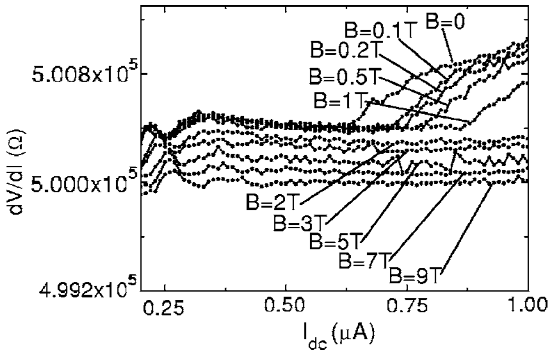

FIG. 3. Differential resistance dV/dI characteristics as a function of the superimposed dc bias current (only the one-way sweep is shown) measured at different magnetic fields and at temperature 10 K in another typical constriction. The shift of the features at higher currents with increasing magnetic field is clearly visible.

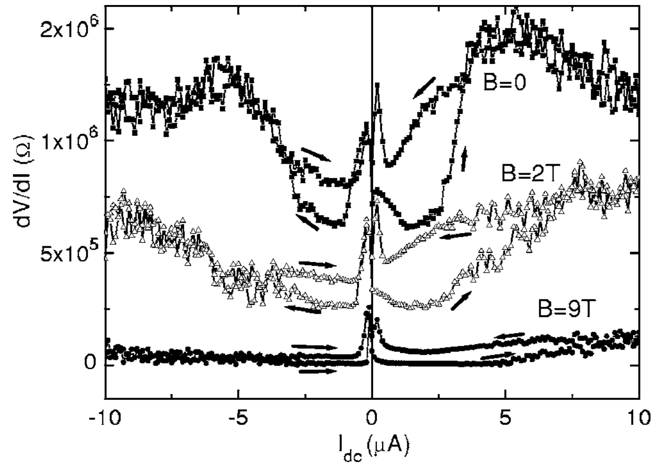

FIG. 4. Differential resistance dV/dI characteristics as a function of the superimposed dc bias current (which is cycled from zero, to its maximum positive value, then to its maximum negative value, then again to zero as indicated by the black arrows) measured at different magnetic fields and at temperature 10 K in an uncostricted mesa. The curves are shifted by a constant offset for clarity.

of Fig. 2(a), there is a smooth resistance rise, indicated by the black arrows, at a certain positive threshold current, encountered in the increasing sweep of the dc bias current. The curves are instead smooth and reversible for bias current of the opposite sign, at least within the noise of the measurement. These smooth steps are not changed when the sign of the magnetic field is inverted. In addition, the sign of the current branch where the steps are present does not depend on which current branch is swept first, as shown in Fig. 2(b), even if the exact shape of the hysteresis itself is obviously altered by the history of the current sweep. On the contrary, the intensity of the magnetic field is effective in shifting the steps at higher currents, as clearly shown in the constriction of Fig. 3. By reverse sweeping the bias current in the opposite direction from high values down to zero, no steps are observed in either the positive or the negative branches of the dV/dI curves. The ac resistance characteristics measured in unconstricted mesas are still strongly asymmetric, but hysteretic features appear also in the opposite branch of bias current, as shown in Fig. 4. Also, the measurements carried out at larger temperature, shown up to 140 K in Fig. 2(c), tend to be more symmetric. The increasing temperature has the further effect of decreasing the threshold current.

This phenomenology is observed in several similar devices of width from 0.1 to 1 μm, but not in all of them; in particular, it was not observed in the less resistive ones.

We suggest that our measurements are a signature of local magnetic moment orientation driven by the spin-polarized dc current, similar to what is suggested in the experiments of Refs. 22, 33, and 23. Indeed, the effect is highly asymmetric with respect to the sign of the bias current and is independent of the sign of the magnetic field; these two characteristics distinguish the magnetization reversal by spin injection from the possible reversal by the magnetic field generated by the current, as well as from domain wall motion by momentum transfer. On the other hand, in general, in constrictions, spin-transfer torque dominates over orientation by the self-field associated with flowing currents (in our geometry the self-field is estimated to be as low as 10^{-7} T).

In Fig. 5, a schematic sketch of adjacent domains along the current path is shown. The resistance changes are related to the rotation of domains whose coercive fields are low enough, that is, domains that are smaller in size. One such domain, indicated by the letter B in Fig. 5, is represented together with two adjacent larger domains A and C. These larger domains A and C have larger coercive fields so that they should be thought of as fixed; instead, the domain B is able to rotate under the effect of the torques $\boldsymbol{\tau}_{\mathbf{A}}$, due to polarized carriers coming from the domain A, and $\boldsymbol{\tau}_{\mathbf{C}}$, due to polarized carriers going toward the domain C. The charge carriers flow is assumed to be from right to left (in the opposite case all the signs of the torques should be reversed). The expressions for the torques $\boldsymbol{\tau}_{\mathbf{A}}$ and $\boldsymbol{\tau}_{\mathbf{C}}$ are proportional to the vectorial products

$$\boldsymbol{\tau}_{\mathbf{A}} \propto I_{AB}\mathbf{s_B} \times (\mathbf{s_B} \times \mathbf{s_A}), \quad \boldsymbol{\tau}_{\mathbf{C}} \propto I_{CB}\mathbf{s_B} \times (\mathbf{s_B} \times \mathbf{s_C}),$$

where $\mathbf{s_A}$, $\mathbf{s_B}$, and $\mathbf{s_C}$ are the unit vectors in the direction of the local magnetic moment of each grain and the electric currents I_{AB} from A to B and I_{CB} from C to B are expressed with their sign, so that in Fig. 5, I_{AB} and I_{CB} have opposite signs. In other words, the torque $\boldsymbol{\tau}_{\mathbf{A}}$ always tends to move the domain B toward the direction of A, whereas the torque $\boldsymbol{\tau}_{\mathbf{C}}$ always tends to rotate B away from C. Now, depending on the initial configuration of the domains, different possibilities exist. In the two upper panels of Fig. 5, the domains are almost parallel to one another in their initial configuration, but in the first panel, $\boldsymbol{\tau}_{\mathbf{A}}$ and $\boldsymbol{\tau}_{\mathbf{C}}$ point toward the same direction, while in the second panel they act oppositely to each other. Thereby, in the case of the first panel, the domain B rotates in such a way that the domain wall resistance AB decreases and the domain wall resistance BC increases, so that the overall effect depends on the total domain wall cross section of one type along the current path with respect to the other domain wall type. In the case of the second panel, instead, the resulting torque on B vanishes and the overall domain wall resistances remain almost unchanged. Similar situations are sketched in panels 3 and 4 of Fig. 5, with an

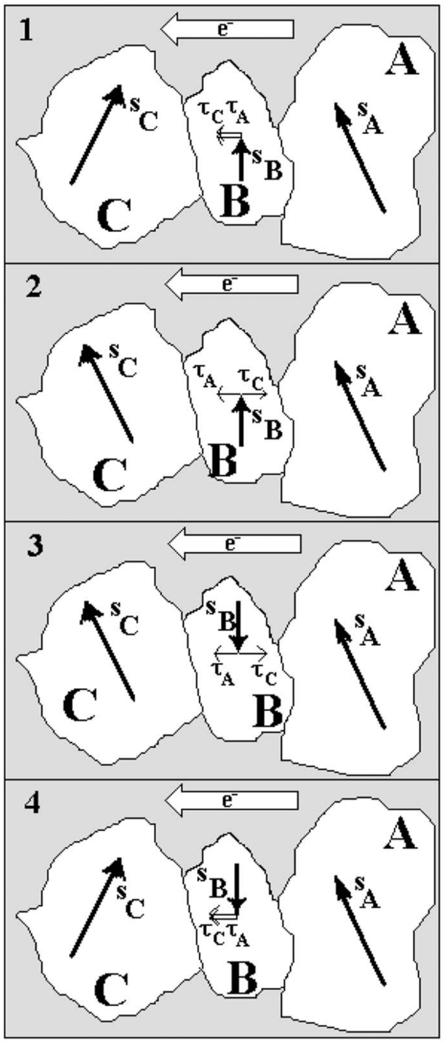

FIG. 5. Schematic picture of adjacent magnetic domains in four different initial configurations. The polarized electron flow is assumed from right to left (in the opposite case all the signs of the torques should be reversed). The thick arrows $\mathbf{s_A}$, $\mathbf{s_B}$, and $\mathbf{s_C}$ indicate the direction of each domain magnetization. The larger domains A and C have larger coercive fields than the smaller domain B, so that only the latter rotates, due to the spin torques $\boldsymbol{\tau}_\mathbf{A}$ and $\boldsymbol{\tau}_\mathbf{C}$. The torque $\boldsymbol{\tau}_\mathbf{A}$ is due to the electrons tunneling from the domain A to the domain B, while the torque $\boldsymbol{\tau}_\mathbf{C}$ is due to the electrons tunneling from the domain B to the domain C. The directions and signs of $\boldsymbol{\tau}_\mathbf{A}$ and $\boldsymbol{\tau}_\mathbf{C}$ are determined by the direction of the charge-carrier flow and by the direction of the local magnetization of the adjacent domains, according to the theory of spin torque.

initial configuration of nearly antiparallel domains; indeed, the parallel or antiparallel equilibrium configuration, depends on the sign of the exchange interaction, which in turn is determined by the height of the energy barrier between the domains.[43] Again, since the torque $\boldsymbol{\tau}_\mathbf{A}$ moves the domain B toward the direction of A, and the torque $\boldsymbol{\tau}_\mathbf{C}$ rotates B away from C, it turns out that, in panel 3, the wall resistances are almost unchanged, whereas, in panel 4, the domain wall resistance AB decreases and the domain wall resistance BC increases. This argument shows that this effect is intrinsically dependent on the sign of the bias current, but also that, if multiple domains and current paths are present, both signs of the current may be active in rotating the domains, yielding resistive changes. In the limiting case that the resistance is dominated by a single domain wall at the constriction (imagine that only two domains, say A and B, exist and neglect the domain C), the effect is asymmetric with respect to the sign of the bias current. On the other hand, if the measurement is carried out in unconstricted areas or at larger temperatures, where more and smaller magnetic domains are present, a symmetric effect is expected on average. This agrees very well with our experimental observations. Therefore, in our description of the system, at low current bias the adjacent domains along the current path are almost parallel, as in panel 1 of Fig. 5; if the bias current is negative, the spin torque tends to align them further with almost no change in the measured resistance (as it would occur to the domain wall resistance AB in panel 1 for electrons flowing from right to left), while if the bias current is positive, it tends to increase their misalignment angle so that the measured resistance increases (as it would occur to the domain wall resistance AB in panel 1 for electrons flowing from left to right). The magnetic field favors the domain orientation parallel to its direction and competes with the spin torque when the latter forces the antiparallel alignment, thus increasing the threshold current for the appearance of the features, as it is evident in Fig. 3. In unconstricted mesas, shown in Fig. 4, the measurements exhibit features for both signs of the bias current as a consequence of the larger number of available metallic domains along the current path, having both higher and smaller coercive fields. This situation is some similar to what was observed in measurements performed in constrictions at high temperature, shown in Fig. 2(c): close to the metal-insulator transition, there may be a larger number of smaller magnetic domains and/or larger conductance across the barriers between them; as a consequence, the current encounters domains with a broad range of coercive field values along its paths, so that the curves become more symmetric with respect to the sign of the current. The increased temperature also has the effect of lowering the threshold current, possibly because it provides the activation energy for domains rotation, as shown in Fig. 2(c).

The hysteretic behavior of Fig. 2 is interpreted as follows. Starting from negative bias current, the parallel alignment is stabilized and the resistance is nearly constant. When the bias dc current becomes positive, the spin torque tends to rotate the domains with smaller coercive field toward antiparallel configurations. The resistance thus increases with an increasing misalignment angle between the domains. Indeed, the energy bands of misaligned domains are displaced in energy with respect to each other, so that an energy cost up to $\sim$2 eV, which is the Hund's splitting in manganites,[44] has to be paid for a charge carrier to be injected from one domain to the other. When sweeping backward the dc bias current from its maximum value down to zero, the resistance maintains its higher value; this determines the hysteretic behavior and indicates that the domains lag in their misaligned configuration, with consequent dissipation. When crossing zero dc bias current the domains gradually return to their close-to-parallel equilibrium configuration (it may be that they switch back to the close-to-parallel equilibrium configuration at very low bias currents in the region of the zero bias anomaly whose resistance cannot be measured). If the dc current is swept again to negative values, no features are observed in the resistance curve, which remains in its lower value, consistent with the fact that the negative current stabilizes the parallel alignment.

We note that our findings are not compatible with a picture where the electric field triggers the formation of filamentary conducting paths of ferromagnetic clusters;[24,28,20] first, in our case the current yields a resistivity increase and not a decrease; second, the magnetic field enhances the current threshold, instead of lowering it. Neither role of the metal-oxide interfacial areas[19] can be directly related to our experiments, as evidenced by a comparison between four-probe and three-probe measurements.

The threshold current for the appearance of the features is in the range 10^7-10^8 A/m^2, much smaller than that predicted for metals ($\sim 10^{11}$ A/m^2),[37,38] and also smaller than that observed in magnetic semiconductors (8×10^8 A/m^2).[45] We point out that the percolative nature of transport in our low doped samples makes it difficult to get a realistic value of the local current density. Indeed, the current density calculated assuming a homogeneous cross-section largely underestimates the more realistic effective current density value that is obtained by assuming a transport through metallic clusters; in Refs. 22 and 23, the latter effective value is consistent with our current density values. Also, the current values of Ref. 33 are compatible with ours. Moreover, we note that the polarization of conduction electrons is close to 100% in manganites, whereas it is only a few percent in magnetic semiconductors, so that in our system almost the whole electric current is effective in the spin torque mechanism. We also suggest that Joule heating may play a role in activating domain rotation in this resistive material[46,47,29] (the resistivity of our films at low temperature is of the order of 10^{-4} Ω m, that is, five orders of magnitude larger than the resistivity of typical ferromagnetic metals such as cobalt). In addition, it has been shown that surface spin waves could be excited at threshold currents which can be two orders of magnitude smaller than in the case of bulk spin waves.[48] The calculated current threshold for excitation of surface spin waves is just compatible with our values, assuming input parameters of manganites taken from literature. Finally, a possible role of the small anisotropy magnetic constant K has been proposed to account for low values of the threshold current.[22]

The samples where no features are seen are the less resistive ones where the ferromagnetic phase is well established and the magnetic domains are larger in size with higher coercive fields, so that the threshold current for domain rotation by spin torque is not yet reached in the explored experimental range of currents. Also, Joule heating assisted rotation of domains is obviously less effective in the less resistive constrictions.

In Fig. 6(a), we present dc current-voltage characteristics measured in a similar constriction at 10 K and at different magnetic fields parallel to the film surface. It can be clearly seen that in the positive branches the curves exhibit nonlinear shape in zero and low magnetic fields, while they become increasingly ohmic with increasing field up to 9 T, as already

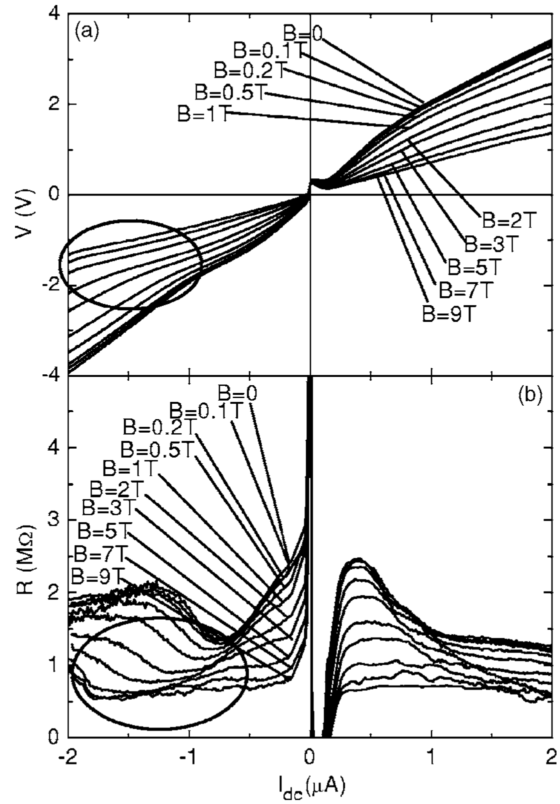

FIG. 6. (a) dc current-voltage characteristics of a constriction measured at different magnetic fields at 10 K. (b) Constriction differential resistance obtained from the curves of the upper panel (a) by numerical differentiation. The ellipses evidence the sharp changes of slope observed for negative sign of the applied current.

observed in a previous report.[11] We think that nonlinearity at zero and low fields is a signature of electron tunneling[49,50] across multiple domain walls and the crossover from nonlinear to linear behavior is related to the progressive disappearance of energy barriers between adjacent magnetic domains along the current path as the external field increases, due to the rotation and merging of magnetic domains. Moreover, as evidenced by a circle, these dc current-voltage characteristics exhibit sharp changes of slope for a certain (negative) sign of current, which are shifted toward high currents with increasing magnetic field. These features are clearly seen in Fig. 6(b) where the constriction differential resistances obtained from the curves of the upper panel of Fig. 5(a) by numerical differentiation are shown. We think that such changes of slope are again due to the spin torque mechanism; indeed, the phenomenology of the kinks is very similar to that of the resistance steps observed in ac resistance characteristics of Figs. 2–4. The above-mentioned divergence of resistance at small current bias is also observed.

IV. CONCLUSIONS

We fabricate submicrometric constrictions in $La_{0.67}Ba_{0.33}MnO_{3-\delta}$ thin films by FIB and carry out ac resistance measurements as a function of a dc bias current and external magnetic field applied in the plane of the film. We observe a hysteretic behavior which is driven not only by the external magnetic field, but also by the polarized dc bias current. Due to the distinctive asymmetry of the curves with respect to the sign of the bias current, we propose an explanation of the observed phenomenology in terms of local magnetic moment orientation by spin torque.

This effect observed in very simple planar devices may be exploited in perspective for current driven and magnetic field sensitive memory elements in spintronics applications. Indeed, we wish to emphasize that the threshold current for the appearance of hysteretic features is in the range $10^7-10^8\ \mathrm{A/m^2}$, which is a fairly low value as compared to those employed in most cobalt-based systems.

ACKNOWLEDGMENTS

The authors acknowledge the financial support of the ESF, through the THIOX program.

*Electronic address: pallecchi@fisica.unige.it

[1] M. Bowen, M. Bibes, A. Barthélémy, J. P. Contour, A. Anane, Y. Lemaître, and A. Fert, Appl. Phys. Lett. **82**, 233 (2003).
[2] J. Z. Sun, W. J. Gallagher, P. R. Duncombe, L. Kursin-Elbaum, R. A. Altman, A. Gupta, Y. Lu, G. Q. Gong, and G. Xiao, Appl. Phys. Lett. **69**, 3266 (1996).
[3] J. Z. Sun, L. Kursin-Elbaum, P. R. Duncombe, A. Gupta, and R. B. Laibowitz, Appl. Phys. Lett. **70**, 1769 (1997).
[4] Y. Lu, X. W. Li, G. Q. Gong, G. Xiao, A. Gupta, P. Lecoeur, J. Z. Sun, Y. Y. Wang, and V. P. Dravid, Phys. Rev. B **54**, R8357 (1996).
[5] J. M. De Teresa, A. Barthélémy, A. Fert, J. P. Contour, F. Montaigne, and P. Seneor, Science **286**, 507 (1999).
[6] J. M. De Teresa, A. Barthélémy, A. Fert, J. P. Contour, R. Lyonnet, F. Montaigne, P. Seneor, and A. Vaurès, Phys. Rev. Lett. **82**, 4288 (1999).
[7] H. Q. Yin, J. S. Zhou, K. Sugawara, and J. B. Goodenough, J. Magn. Magn. Mater. **222**, 115 (2000).
[8] P. Bruno, Phys. Rev. Lett. **83**, 2425 (1999).
[9] N. Garcia, M. Muñoz, and Y. W. Zhao, Phys. Rev. Lett. **82**, 2923 (1999).
[10] O. Pietzsch, A. Kubetzka, M. Bode, and R. Wiesendanger, Phys. Rev. Lett. **84**, 5212 (2000).
[11] I. Pallecchi, E. Bellingeri, G. Canu, A. Caviglia, A. S. Siri, and D. Marré, J. Appl. Phys. **99**, 114508 (2006).
[12] O. Céspedes, S. M. Watts, J. M. D. Coey, K. Dörr, and M. Ziese, Appl. Phys. Lett. **87**, 083102 (2005).
[13] Y. Tomoda, Y. Shibata, J. I. Shirakashi, and Y. Takemura, J. Appl. Phys. **99**, 08T312 (2006).
[14] S. B. Ogale, V. Talyansky, C. H. Chen, R. Ramesh, R. L. Greene, and T. Venkatesan, Phys. Rev. Lett. **77**, 1159 (1996).
[15] M. Ziese, S. Sena, C. Shearwood, H. J. Blythe, M. R. J. Gibbs, and G. A. Gehring, Phys. Rev. B **57**, 2963 (1998).
[16] A. Masuno, T. Terashima, Y. Shimakawa, and M. Takano, Appl. Phys. Lett. **85**, 6194 (2004); T. Wu, S. B. Ogale, J. E. Garrison, B. Nagaraj, A. Biswas, Z. Chen, R. L. Greene, R. Ramesh, T. Venkatesan, and A. J. Millis, Phys. Rev. Lett. **86**, 5998 (2001).
[17] I. Pallecchi, L. Pellegrino, E. Bellingeri, A. S. Siri, and D. Marré, Appl. Phys. Lett. **83**, 4435 (2003).
[18] X. Hong, A. Posadas, A. Lin, and C. H. Ahn, Phys. Rev. B **68**, 134415 (2003).
[19] S. Tsui, A. Baikalov, J. Cmaidalka, Y. Y. Sun, Y. Q. Wang, Y. Y. Xue, C. W. Chu, L. Chen, and J. Jacobson, Appl. Phys. Lett. **85**, 317 (2004); M. Quintero, A. G. Leyva, and P. Levy, *ibid.* **86**, 242102 (2005); A. Baikalov, Y. Q. Wang, B. Shen, B. Lorenz, S. Tsui, Y. Y. Sun, Y. Y. Xue, and C. W. Chu, *ibid.* **83**, 957 (2003).
[20] S. Q. Liu, N. J. Wu, and A. Ignatiev, Appl. Phys. Lett. **76**, 2749 (2000).
[21] Y. Tokunaga, Y. Kaneko, J. P. He, T. Arima, A. Sawa, T. Fujii, M. Kawasaki, and Y. Tokura, Appl. Phys. Lett. **88**, 223507 (2006).
[22] Y. Yuzhelevski, V. Markovich, V. Dikovsky, E. Rozenberg, G. Gorodetsky, G. Jung, D. A. Shulyatev, and Y. M. Mukovskii, Phys. Rev. B **64**, 224428 (2001).
[23] J. Z. Sun, J. Magn. Magn. Mater. **202**, 157 (1999).
[24] A. Asamitsu, Y. Tomioka, H. Kuwahara, and Y. Tokura, Nature (London) **388**, 50 (1997).
[25] C. N. R. Rao, A. R. Raju, V. Ponnambalam, S. Parashar, and N. Kumar, Phys. Rev. B **61**, 594 (2000).
[26] K. Hatsuda, T. Kimura, and Y. Tokura, Appl. Phys. Lett. **83**, 3329 (2003).
[27] S. Mercone, A. Wahl, Ch. Simon, and C. Martin, Phys. Rev. B **65**, 214428 (2002).
[28] A. Guha, A. K. Raychaudhuri, A. R. Raju, and C. N. R. Rao, Phys. Rev. B **62**, 5320 (2000).
[29] A. S. Carneiro, R. F. Jardim, and F. C. Fonseca, Phys. Rev. B **73**, 012410 (2006).
[30] D. Hsu, J. G. Lin, and W. F. Wu, Appl. Phys. Lett. **88**, 222507 (2006).
[31] Y. Tokura and N. Nagaosa, Science **288**, 462 (2000).
[32] Y. F. Chen, M. Ziese, and P. Esquinazi, Appl. Phys. Lett. **88**, 222513 (2006).
[33] J. Gao, S. Q. Shen, T. K. Li, and J. R. Sun, Appl. Phys. Lett. **82**, 4732 (2003).
[34] E. B. Myers, D. C. Ralph, J. A. Katine, R. N. Louie, and R. A. Buhrman, Science **285**, 867 (1999).
[35] T. Y. Chen, Y. Ji, and L. Chien, Appl. Phys. Lett. **84**, 380 (2004).
[36] J. A. Katine, F. J. Albert, R. A. Buhrman, E. B. Myers, and D. C. Ralph, Phys. Rev. Lett. **84**, 3149 (2000).
[37] J. Shibata, G. Tatara, and H. Kohno, Phys. Rev. Lett. **94**, 076601 (2005).
[38] Z. Li and S. Zhang, Phys. Rev. Lett. **92**, 207203 (2004).
[39] L. Berger, J. Appl. Phys. **55**, 1954 (1984).
[40] L. Berger, J. Appl. Phys. **71**, 2721 (1992).
[41] J. C. Slonczewski, J. Magn. Magn. Mater. **159**, L1 (1996).
[42] Ll. Balcells, J. Fontcuberta, B. Martínez, and X. Obradors, Phys. Rev. B **58**, R14697 (1998).
[43] J. C. Slonczewski, Phys. Rev. B **39**, 6995 (1989).
[44] Y. Okimoto, T. Katsufuji, T. Ishikawa, T. Arima, and Y. Tokura, Phys. Rev. B **55**, 4206 (1997).
[45] M. Yamanouchi, D. Chiba, F. Matsukura, and H. Ohno, Nature (London) **428**, 539 (2004).
[46] E. B. Myers, F. J. Albert, J. C. Sankey, E. Bonet, R. A. Buhrman,

and D. C. Ralph, Phys. Rev. Lett. **89**, 196801 (2002).
[47] J. Gao, S. Q. Shen, T. K. Li, and J. R. Sun, Appl. Phys. Lett. **82**, 4732 (2003); Y. G. Zhao, Y. H. Wang, G. M. Zhang, B. Zhang, X. P. Zhang, C. X. Yang, P. L. Lang, M. H. Zhu, and P. C. Guan, *ibid.* **86**, 122502 (2005); F. X. Hu and J. Gao, Phys. Rev. B **69**, 212413 (2004).
[48] Z. Li, J. He, and S. Zhang, J. Appl. Phys. **99**, 08Q702 (2006).
[49] J. G. Simmons, J. Appl. Phys. **34**, 1793 (1963).
[50] T. Kiyomura, Y. Maruo, and M. Gomi, J. Appl. Phys. **88**, 4768 (2000).